STRUCTURAL BIOLOGY COMMUNICATIONS

ISSN 2053-230X

The periplasmic sensing domain of *Vibrio fischeri* chemoreceptor protein A (VfcA): cloning, purification and crystallographic analysis

Abu Iftiaf Md Salah Ud-Din[a] and Anna Roujeinikova[a,b]*

[a]Infection and Immunity Program, Monash Biomedical Discovery Institute and Department of Microbiology, Monash University, Wellington Road, Clayton, Victoria 3800, Australia, and [b]Department of Biochemistry and Molecular Biology, Monash University, Wellington Road, Clayton, Victoria 3800, Australia. *Correspondence e-mail: anna.roujeinikova@monash.edu

Received 24 February 2016
Accepted 8 April 2016

Edited by Z. Dauter, Argonne National Laboratory, USA

Keywords: bacterial chemotaxis; receptor; sensing domain; methyl-accepting protein.

Flagella-mediated motility and chemotaxis towards nutrients are important characteristics of *Vibrio fischeri* that play a crucial role in the development of its symbiotic relationship with its Hawaiian squid host *Euprymna scolopes*. The *V. fischeri* chemoreceptor A (VfcA) mediates chemotaxis toward amino acids. The periplasmic sensory domain of VfcA has been crystallized by the hanging-drop vapour-diffusion method using polyethylene glycol 3350 as a precipitating agent. The crystals belonged to space group *P*1, with unit-cell parameters $a = 39.9$, $b = 57.0$, $c = 117.0$ Å, $\alpha = 88.9$, $\beta = 80.5$, $\gamma = 89.7^\circ$. A complete X-ray diffraction data set has been collected to 1.8 Å resolution using cryocooling conditions and synchrotron radiation.

1. Introduction

The marine bacterium *Vibrio fischeri* forms mutualistic and pathogenic interactions with animal hosts (Nealson & Hastings, 1991). *V. fischeri* exists in two forms: (i) a free-living organism in the gut of many marine mammals and (ii) a light-organ symbiont in certain species of squid and fish (Nealson & Hastings, 1991).

Bacterial flagella-mediated motility and chemotaxis are crucial for the establishment of symbiotic relationships between bacteria and other organisms (Manson *et al.*, 1998; Norsworthy & Visick, 2013; Sourjik & Wingreen, 2012). Chemotaxis appears to play a role in guiding *V. fischeri* towards the colonization-permissive sites in its symbiotic Hawaiian squid host *Euprymna scolopes* (Norsworthy & Visick, 2013). Membrane-embedded methyl-accepting chemotaxis proteins (MCPs) serve as receptors that recognize chemoattractants or repellents. Upon ligand binding, MCPs transduce the signal through the CheAY two-component system to guide bacterial motility toward chemoattractants and away from repellents (Norsworthy & Visick, 2013). Of the 43 putative MCPs encoded in the genome of *V. fischeri*, the involvement in chemotaxis has been so far studied for three: VfcA (*V. fischeri* chemoreceptor A), VfcB and VfcB2 (Nikolakakis *et al.*, 2016; Brennan *et al.*, 2013). VfcA mediates chemotaxis towards four amino acids (serine, alanine, cysteine and threonine), while both VfcB and VfcB2 are responsible for mediating chemoattraction to short-chain and medium-chain fatty acids (Norsworthy & Visick, 2013; Brennan *et al.*, 2013). Previous mutagenesis studies have suggested that *vfcA* mutant *V. fischeri* is defective in amino-acid chemotaxis (Brennan *et al.*, 2013).

The mechanism by which VfcA recognizes its signal molecules and the structural basis behind its ligand specificity remain unknown. A *BLAST* search against the known structures available in the Protein Data Bank (PDB) revealed that the periplasmic sensing domain of VfcA (VfcA^{peri}) has less than 26% amino-acid sequence homology to any structurally characterized receptor [25 and 20% sequence similarity to the *V. cholerae* chemoreceptor MCP37 (PDB entry 3c8c; New York SGX Research Center for Structural Genomics, unpublished work) and to histidine kinase from *Methanosarcina mazei* (PDB entries 3li8, 3li9, 3lia and 3lib; Zhang & Hendrickson, 2010), respectively]. According to a Pfam analysis (Finn *et al.*, 2016) of its primary sequence, VfcA contains a Cache_1 (calcium channels and chemotaxis receptors) motif located between residues 107 and 185 (Anantharaman & Aravind, 2001) and thus belongs to the family of tandem Per–Arnt–Sim (tandem PAS) sensing domains. We have recently reported the crystal structure of the periplasmic domain of *Campylobacter jejuni* Tlp3 (22% amino-acid sequence identity to VfcA^{peri}), which is a different member of the family of MCP receptors for amino acids that contains a tandem PAS sensing domain (Liu *et al.*, 2015). To investigate whether members of this family share a common mechanism of amino-acid recognition, we have initiated structural studies on VfcA^{peri}. Here, we report the expression, purification and co-crystallization of VfcA^{peri} with one of its putative signal molecules.

2. Materials and methods

2.1. Cloning, protein expression and purification

The two transmembrane helices of VfcA from *V. fischeri* strain ES114 (UniProtKB Q5E6S4) were predicted to comprise residues 7–25 and 273–296 using the *TMHMM* server v.2.0 (http://www.cbs.dtu.dk/services/TMHMM-2.0/; Krogh *et al.*, 2001; Fig. 1). The *Escherichia coli* codon-optimized DNA fragment encoding the periplasmic sensory domain of VfcA (VfcA^{peri}; amino-acid residues 26–272) was synthesized and ligated into the expression vector pET151/D-TOPO (Invitrogen) by GenScript.

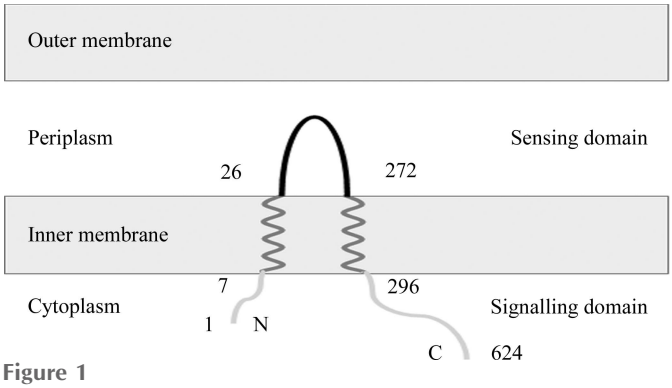

Figure 1
The predicted membrane topology of VfcA and the boundaries (amino-acid residue numbers) of the periplasmic sensory domain VfcA^{peri} characterized in this study.

The recombinant protein used for crystallization comprised residues 26–272 of VfcA plus six additional residues (GIDPFT) originating from the *Tobacco etch virus* (TEV) protease cleavage site and vector. The recombinant VfcA^{peri} was expressed in *E. coli* BL21 (DE3) cells (Novagen) grown at 37°C in Luria–Bertani broth containing 50 mg l^{-1} ampicillin (Aspen Pharmacare) to an $OD_{600\ nm}$ of 0.6 and then induced with 0.5 m*M* isopropyl β-D-1-thiogalactopyranoside (Thermo Scientific) for 3.5 h. The cells were harvested, resuspended in a buffer consisting of 20 m*M* Tris–HCl pH 8.0, 100 m*M* NaCl, 1 m*M* phenylmethylsulfonyl fluoride and lysed using an EmulsiFlex-C5 high-pressure homogenizer (Avestin). The cell lysate was clarified by centrifugation at 12 000*g* for 30 min at 4°C. NaCl and imidazole were then added to the supernatant to final concentrations of 500 and 15 m*M*, respectively, before loading it onto a 5 ml HiTrap Chelating HP column (GE Healthcare) pre-washed with buffer *A* (20 m*M* Tris–HCl pH 8.0, 500 m*M* NaCl, 20 m*M* imidazole). The column was washed with 20 column volumes of buffer *A* and the protein was eluted with buffer *A* supplemented with 500 m*M* imidazole. The His_6 tag was cleaved with His_6-TEV protease (Invitrogen) whilst dialyzing the sample overnight at 4°C against buffer *B* [50 m*M* Tris–HCl pH 8.0, 2 m*M* dithiothreitol, 200 m*M* NaCl, 1%(*v*/*v*) glycerol]. NaCl and imidazole were then added to the sample to final concentrations of 500 and 20 m*M*, respectively, and the TEV protease and the uncleaved protein were removed by passing the sample through a HiTrap Chelating HP column. The flowthrough fractions were collected and concentrated to 2 ml in a Vivaspin 10 kDa cutoff concentrator and further purified by passing them through a Superdex 200 HiLoad 26/60 gel-filtration column (GE Healthcare) equilibrated with buffer *C* (10 m*M* Tris–HCl pH 8.0, 200 m*M* NaCl). The protein was concentrated to 10 mg ml^{-1} (the concentration was determined using the Bradford assay; Bradford, 1976). The protein purity was estimated to be greater than 98% by quantifying the protein in the VfcA band and the

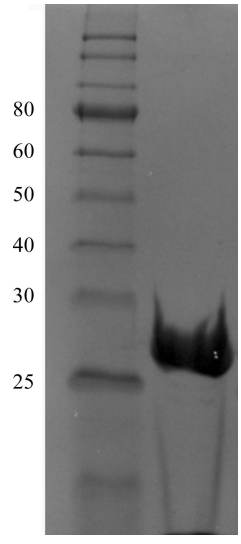

Figure 2
Coomassie Blue-stained 12% SDS–PAGE gel of recombinant VfcA^{peri}. The left lane contains molecular-weight marker (labelled in kDa).

impurities on an SDS–PAGE gel with *ImageJ* (https://imagej.nih.gov/ij/; Fig. 2). The oligomeric state of VfcA^{peri} was calculated using a calibration plot of log(molecular weight) *versus* retention volume [$V_{retention}$ (ml) = 549.3–73.9 × log(molecular weight)] available at the EMBL Protein Expression and Purification Core Facility website (http://www.embl.de/pepcore/pepcore_services/protein_purification/chromatography/hiload26-60_superdex200/index.html).

2.2. Crystallization

Prior to crystallization, VfcA (10 mg ml^{-1}) was mixed with alanine (final concentration 5 m*M*) and then centrifuged for 20 min at 13 000*g* to clarify the solution. The search for crystallization conditions was performed using commercially available screens. The initial crystallization droplets consisted of 100 nl protein solution mixed with 100 nl reservoir solution and equilibrated against 50 µl reservoir solution in a 96-well Art Robbins CrystalMation Intelli-Plate (Hampton Research). Crystals appeared after 1 d from condition No. 79 of Index Screen HT (Fig. 3), which consisted of 200 m*M* ammonium acetate, 100 m*M* bis-tris pH 6.5, 25%(*w*/*v*) polyethylene glycol (PEG) 3350. This condition was further optimized to improve the crystal quality, yielding an optimal crystallization reservoir solution consisting of 200 m*M* ammonium acetate, 100 m*M* HEPES pH 7.0, 25%(*w*/*v*) PEG 3350. Crystallization conditions are detailed in Table 1.

2.3. Data collection and processing

The crystals were briefly soaked in a cryostabilizing solution consisting of 220 m*M* ammonium acetate, 120 m*M* HEPES pH 7.0, 25%(*w*/*v*) PEG 3350, 10 m*M* alanine, 10%(*v*/*v*) glycerol and flash-cooled in liquid nitrogen prior to data collection. X-ray diffraction data were collected to 1.8 Å resolution on the MX1 beamline of the Australian Synchrotron (AS; Fig. 4). A total of 360 images were collected using a 0.5° oscillation width. The data were processed and scaled using *iMosflm* (Battye *et al.*, 2011) and *AIMLESS* (Evans & Murshudov, 2013) from the *CCP*4 suite (Winn *et al.*, 2011). Calculation of the self-rotation function was performed using *POLARRFN* (Winn *et al.*, 2011). The statistics of data collection are summarized in Table 2.

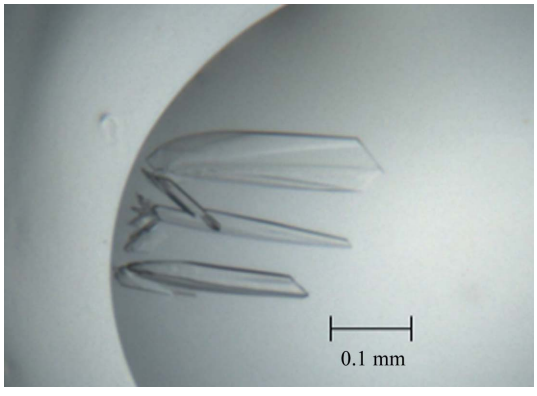

Figure 3
Crystals of a putative complex of VfcA^{peri} with alanine.

Table 1
Crystallization.

Method	Hanging-drop vapour diffusion
Plate type	96-well Art Robbins CrystalMation Intelli-Plate (Hampton Research)
Temperature (K)	293
Protein concentration (mg ml^{-1})	10
Buffer composition of protein solution	100 m*M* ammonium acetate, 12.5%(*w*/*v*) PEG 3350, 50 m*M* HEPES pH 7.0
Composition of reservoir solution	200 m*M* ammonium acetate, 25%(*w*/*v*) PEG 3350, 100 m*M* HEPES pH 7.0
Volume and ratio of drop	1 µl, 1:1
Volume of reservoir (µl)	500

3. Results and discussion

Recombinant VfcA^{peri} was overexpressed in *E. coli* BL21 (DE3) cells harbouring the pET151/D-TOPO plasmid upon induction with T7 polymerase. The protein was purified to >98% electrophoretic homogeneity based on Coomassie Blue staining of SDS–PAGE gels. The recombinant protein consisted of amino-acid residues 27–272 of VfcA^{peri} with six additional amino acids (GIDPFT) at the N-terminus originating from the TEV cleavage site and expression vector. The protein migrated on SDS–PAGE with an apparent molecular weight of 27 kDa, which is close to the value calculated from the amino-acid sequence (27.7 kDa). When subjected to gel filtration, the protein eluted as a single peak with an apparent

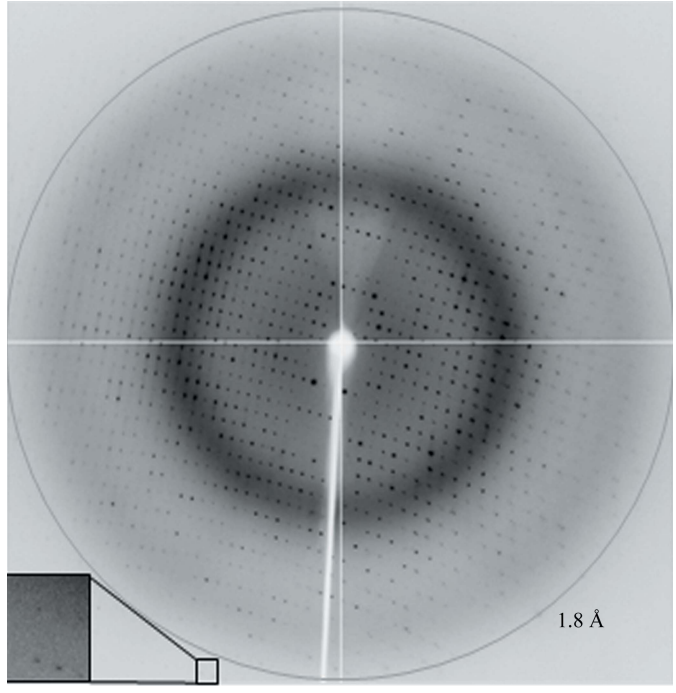

Figure 4
A representative 0.5° oscillation image of the data collected using an ADSC Quantum 210r CCD detector at station MX1, Australian Synchrotron, Victoria, Australia. The magnified rectangle shows diffraction spots beyond the 1.8 Å resolution ring.

Table 2
Data collection and processing.

Values in parentheses are for the outer shell.

Diffraction source	MX1 beamline, AS
Wavelength (Å)	1.0
Temperature (K)	100
Detector	ADSC Quantum 210r
Rotation range per image (°)	0.5
Total rotation range (°)	180
Exposure time per image (s)	1.0
Space group	*P*1
a, *b*, *c* (Å)	39.9, 57.0, 117.0
α, β, γ (°)	88.9, 80.5, 90.0
Mosaicity (°)	0.4
Resolution range (Å)	41.0–1.8 (1.9–1.8)
Total No. of reflections	169704 (7009)
No. of unique reflections	86241 (3821)
Completeness (%)	96 (81)
Multiplicity	2.0 (1.8)
$\langle I/\sigma(I)\rangle$	12.5 (3.9)
$R_{\rm r.i.m.}$	0.075 (0.223)
Overall *B* factor from Wilson plot (Å^2)	15.6

molecular weight of approximately 27 kDa, indicating that VfcA$^{\rm peri}$ is monomeric in solution. This result is consistent with previous reports on other tandem PAS sensing domains, which also behave as monomers in solution (Rico-Jiménez *et al.*, 2013; Machuca, Liu & Roujeinikova, 2015; Machuca, Liu, Beckham *et al.*, 2015; Liu *et al.*, 2015).

Crystals of VfcA$^{\rm peri}$ were obtained in the presence of its putative ligand (alanine) using a sparse-matrix crystallization approach. Images collected from a cryocooled crystal at the Australian Synchrotron showed diffraction to 1.8 Å resolution (Fig. 4). Analysis of the X-ray diffraction data using the autoindexing routine in *iMosflm* is consistent with a *P* triclinic crystal system (space group *P*1), with unit-cell parameters $a = 39.9$, $b = 57.0$, $c = 117.0$ Å, $\alpha = 88.9$, $\beta = 80.5$, $\gamma = 89.7^\circ$. The average $I/\sigma(I)$ value is 12.5 for all reflections (resolution range 41.0–1.8 Å) and 3.9 in the highest resolution shell (1.9–1.8 Å). A total of 169 704 measurements were made of 86 241 independent reflections. Data processing gave an $R_{\rm p.i.m.}$ of 0.075 for intensities (0.223 in the 1.9–1.8 Å resolution shell) and the data were 96% complete (81% completeness in the highest resolution shell).

Calculations of the Matthews coefficient (Matthews, 1977) for two, three and four molecules in the asymmetric unit gave values of 4.7, 3.2 and 2.4 Å^3 Da^{-1}, corresponding to solvent contents of approximately 74, 61 and 48%, respectively. These values fall within the range observed for protein crystals by Matthews (1977). Analysis of the intensity distribution using the *phenix.xtriage* program (Adams *et al.*, 2010) resulted in a multivariate *Z*-score of 3.95 from the *L*-test, which was higher than the value expected for untwinned data (3.5) and suggested the presence of pseudo-merohedral twinning with operators (h, $-k$, $h - l$; $-h$, k, $-l$; $-h$, $-k$, $-h + l$). A self-rotation function calculated by *POLARRFN* using diffraction data between 10 and 5 Å resolution and an integration radius of 25 Å showed no dominant features that could be confidently assigned to noncrystallographic axes. Thus, we are currently unable to determine the protein content of the asymmetric unit. Phasing by molecular replacement has not been possible owing to the low sequence similarity to known structures deposited in the PDB. A search for heavy-atom derivatives and the solution of the structure using multiple isomorphous replacement and/or multiwavelength anomalous dispersion methods is under way.

Acknowledgements

Part of this research was undertaken on the MX1 beamline of the AS, Victoria, Australia. We thank the AS staff for their assistance with data collection. We are also grateful to Dr Danuta Maksel and Dr Robyn Gray at the Monash University Protein Crystallography Unit for assistance with the robotic crystallization trials.

References

Adams, P. D. *et al.* (2010). *Acta Cryst.* D**66**, 213–221.
Anantharaman, V. & Aravind, L. (2001). *Trends Biochem. Sci.* **26**, 579–582.
Battye, T. G. G., Kontogiannis, L., Johnson, O., Powell, H. R. & Leslie, A. G. W. (2011). *Acta Cryst.* D**67**, 271–281.
Bradford, M. M. (1976). *Anal. Biochem.* **72**, 248–254.
Brennan, C. A., DeLoney-Marino, C. R. & Mandel, M. J. (2013). *Appl. Environ. Microbiol.* **79**, 1889–1896.
Evans, P. R. & Murshudov, G. N. (2013). *Acta Cryst.* D**69**, 1204–1214.
Finn, R. D., Coggill, P., Eberhardt, R. Y., Eddy, S. R., Mistry, J., Mitchell, A. L., Potter, S. C., Punta, M., Qureshi, M., Sangrador-Vegas, A., Salazar, G. A., Tate, J. & Bateman, A. (2016). *Nucleic Acids Res.* **44**, D279–D285.
Krogh, A., Larsson, B., von Heijne, G. & Sonnhammer, E. L. (2001). *J. Mol. Biol.* **305**, 567–580.
Liu, Y. C., Machuca, M. A., Beckham, S. A., Gunzburg, M. J. & Roujeinikova, A. (2015). *Acta Cryst.* D**71**, 2127–2136.
Machuca, M. A., Liu, Y. C., Beckham, S. A. & Roujeinikova, A. (2015). *Acta Cryst.* F**71**, 211–216.
Machuca, M. A., Liu, Y. C. & Roujeinikova, A. (2015). *Acta Cryst.* F**71**, 110–113.
Manson, M. D., Armitage, J. P., Hoch, J. A. & Macnab, R. M. (1998). *J. Bacteriol.* **180**, 1009–1022.
Matthews, B. W. (1977). *The Proteins*, 3rd ed., edited by H. Neurath & R. L. Hill, Vol. 3, pp. 468–477. New York: Academic Press.
Nealson, K. & Hastings, J. (1991). *The Prokaryotes*, edited by A. Balows, H. G. Trüper, M. Dworkin, W. Harder & K.-H. Schleifer, pp. 625–639. Berlin, Heidelberg, New York: Springer.
Nikolakakis, K., Monfils, K., Moriano-Gutierrez, S., Brennan, C. & Ruby, E. (2016). *Appl. Environ. Microbiol.* **82**, 696–704.
Norsworthy, A. N. & Visick, K. L. (2013). *Front. Microbiol.* **4**, 356.
Rico-Jiménez, M., Muñoz-Martínez, F., García-Fontana, C., Fernandez, M., Morel, B., Ortega, Á., Ramos, J. L. & Krell, T. (2013). *Mol. Microbiol.* **88**, 1230–1243.
Sourjik, V. & Wingreen, N. S. (2012). *Curr. Opin. Cell Biol.* **24**, 262–268.
Winn, M. D. *et al.* (2011). *Acta Cryst.* D**67**, 235–242.
Zhang, Z. & Hendrickson, W. A. (2010). *J. Mol. Biol.* **400**, 335–353.